MICROMECHANICAL MODELING OF DUCTILE TEARING PHENOMENA

S.Mariani and A.Corigliano

Department of Structural Engineering, Politecnico di Milano
Piazza Leonardo da Vinci 32, 20133, Milan, ITALY

ABSTRACT

In this paper we present results obtained via a newly formulated constitutive model for orthotropic porous-plastic solids which is able to take into account microstructure evolution during finite-strain deformation processes. The microstructural geometry is described by means of an elliptic-cylindrical Representative Volume Element (RVE) containing a coaxial cylindrical cavity; at the macroscopic level, the internal state variables that are assumed to govern the microstructure distortion are the void volume fraction and the void aspect ratio in the RVE cross-section. Major enhancements in the description of the degradation of the strength properties in the fracture process zone are elucidated under imposed deformation paths: peak stress values (beyond which softening takes place in the cavitating solid), stress state triaxiality and internal state variable evolution are presented for voids with different initial aspect ratios in an elastic perfectly-plastic matrix material obeying associative J_2 flow theory of plasticity. These results are compared to those obtained by describing the behaviour of the void-containing material by means of the transversely isotropic Gurson's model.

INTRODUCTION

Ductile tearing phenomena in metals constitute the macroscopic result of a micromechanical process of (micro)void nucleation and growth to coalescence [1, 2, 3]. Elastic-brittle inclusions, of spheroidal or cylindrical shape, trigger the onset of strain localization and, subsequently, diffuse damage mechanisms in the formerly fully-dense matrix material. Void nucleation takes place at the inclusion-matrix interfaces and is related to bonding micro-defects; on the other hand, void coalescence takes place at the ultimate stage of the void growth and interaction phenomenon and is due to the break-down of the microligaments between neighbouring voids. This latter stage starts at high values of the void volume fraction f, that is for high values of the ratio between the volume of voids within a sample material element and the whole sample volume: usually $f \cong 0.2 \div 0.25$ is considered an upper bound for theories that disregard void coalescence.

In this paper the above described behaviour of a progressively cavitating solid is simulated through a constitutive model for orthotropic porous-plastic solids with cylindrical microstructure recently proposed by the Authors [4, 5, 6]. To set a term of comparison, responses obtained via the transversely isotropic Gurson's constitutive law [1, 2] are also presented under the same loading conditions.

The results shown in what follows have been obtained for a binary (composite) material which comprises in the initial unstressed state a matrix obeying associative J_2 flow theory of plasticity and microvoids process). The void-containing material is characterized by means of a cylindrical RVE with elliptic cross-section containing a coaxial and confocal cylindrical void: by applying the kinematic approach of limit analysis to this RVE one gets an (analytical) upper bound for the overall strength of the matrix-void aggregate and the evolution laws for the internal state variables that describe the microstructural geometry.

The major enhancement of the proposed orthotropic constitutive law with respect to the transversely isotropic Gurson's model is the capability to describe the microstructure evolution in a much more accurate way: this is accomplished by introducing a further geometric internal state variable, the void aspect ratio in the RVE cross-section (see below).

It will be shown that microstructure distortion under predominantly deviatoric states of stress can be accounted for in a proper manner; it has to be noticed, in fact, that the overall strength properties of the void-matrix aggregate are extremely sensitive to the microstructural geometry, even at a constant value of the void volume fraction (see [5, 6]).

The results proposed in this paper concern the quantitative evaluation of the degradation of the strength properties in the fracture process zone at finite strains due to void growth and to void distortion. Since plane strain conditions are expected in the central portion of any fracture process zone, the nonlinear material response is checked in the forthcoming numerical examples for different linear (quasi-radial) paths in the plane of the stretch ratios (see [7]) along the principal axes of the elliptic cross-section of the void.

YIELD CRITERIA AND MICROSTRUCTURE EVOLUTION FOR ORTHOTROPIC POROUS-PLASTIC SOLIDS

Let us consider a cylindrical RVE with elliptic cross-section containing a coaxial and confocal elliptic-cylindrical cavity (see Fig. 1); this geometry does not allow to fill the continuum without gaps but is here assumed to approximately represent the actual microstructure of an array of hexagonal cylindrical void-containing RVE with different spacings along the x_1 and x_2 axes in the cross-section plane.

The microstructure can be described by means of two geometrical internal state variables, i.e. the void volume fraction f and the void aspect ratio λ in the RVE cross-section. Making reference to Fig. 1 they are respectively defined as:

$$f = \frac{\pi \frac{b_1 b_2}{4}}{\pi \frac{a_1 a_2}{4}} = \frac{b_1 b_2}{a_1 a_2}, \tag{1}$$

$$\lambda = \frac{b_2}{b_1}. \tag{2}$$

In the above equations a_i and b_i $(i = 1, 2)$ are, respectively, the axis lengths of the ellipses at the outer boundary of the RVE cross-section and at the void-matrix interface aligned with reference axis x_i.

The transversely isotropic Gurson's model was introduced for a subclass of the microstructures here treated, namely for $a_1 = a_2$ and $b_1 = b_2$. λ can thus be properly used to describe the eccentricity of the elliptic-cylindrical void surface and to furnish a measure of the discrepancy from the Gurson's model, which assumes $\lambda = 1$ constant throughout the whole deformation process.

A further internal state variable has to be introduced if voids are allowed to deform under shear loading conditions in the $x_1 - x_2$ plane; this aspect is not addressed here because we assume that the considered RVE is placed in the fracture process zone straight ahead of the current crack tip during a mode I crack propagation process.

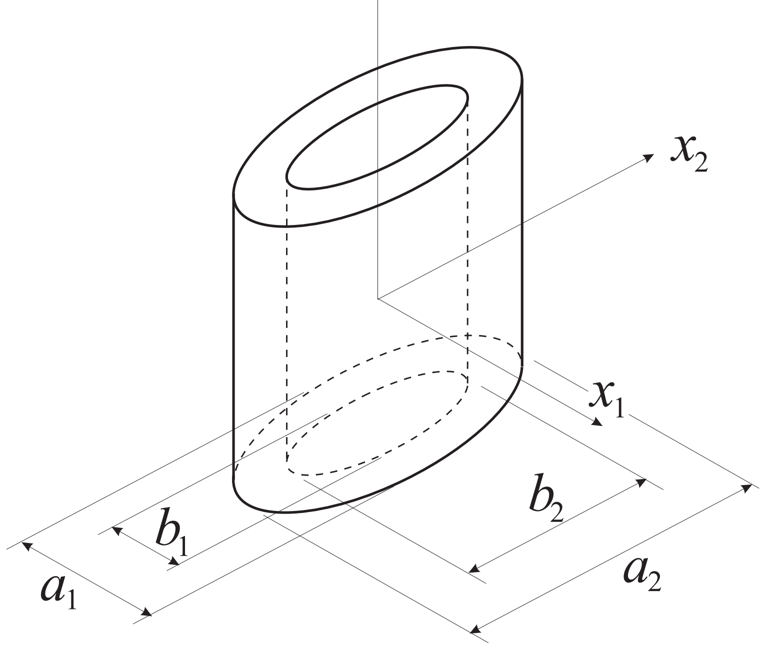

Figure 1. Geometry of the Representative Volume Element

To study at the macroscale the void growth process the overall elastic and strength properties of the RVE are required. In the remainder of this paper a main assumption has been introduced: the elastic moduli of the void-containing solid (see, e.g., [8]) are fixed at their values in the undeformed configuration. This has been conceived in order to simplify the numerical treatment of the problem: if degradation of the elastic stiffness of the solid due to void growth has to be taken into account, a further dissipative mechanism at the macroscale, usually referred to as continuum damage, should be considered along with plasticity.

As far as the homogenized yield condition is concerned, an upper bound for it has been obtained by applying to the RVE the kinematic approach of limit analysis [4, 5]. A simplified velocity field in the matrix volume at plastic collapse is introduced, which respects matrix plastic incompressibility -we recall that the perfectly-plastic matrix material is assumed to obey associative J_2 flow theory of plasticity- and uniform strain rate boundary conditions [9, 10]. For the sake of brevity readers are referred to [5, 6] for details concerning the formulation and numerical time-stepping algorithmic treatment of the proposed constitutive model, which comprises a yield locus (either expressed in terms of stress components in the x_1, x_2, x_3 reference frame or orthotropic invariants of the stress tensor [11]), associated flow rules for the plastic components of the strain rate tensor and evolution laws for the geometric internal state variables f and λ.

Microstructure evolution can thus be studied by exploiting the effects on the RVE geometry of the assumed velocity field at plastic collapse. While the evolution law for f is governed by the conservation of mass principle, the variation of λ is linked to the deviatoric state of stress in the RVE cross-section through a much less simple law. Furthermore, in the next Section it is shown that coupled transversely isotropic elasticity and plasticity can lead to a somewhat surprising evolution of λ under imposed linear paths in the plane of the stretch ratios in the RVE cross-section.

RESULTS

As mentioned in the preceding Section, the response of the orthotropic constitutive law at finite strain is here studied in the absence of shear loading conditions, namely in the case of principal axes of the stress tensor always aligned with reference axes x_1, x_2, x_3. It is thus not necessary to introduce objective rates of the stress tensor, like the Jaumann or the Green-Naghdi ones, to integrate in time the nonlinear

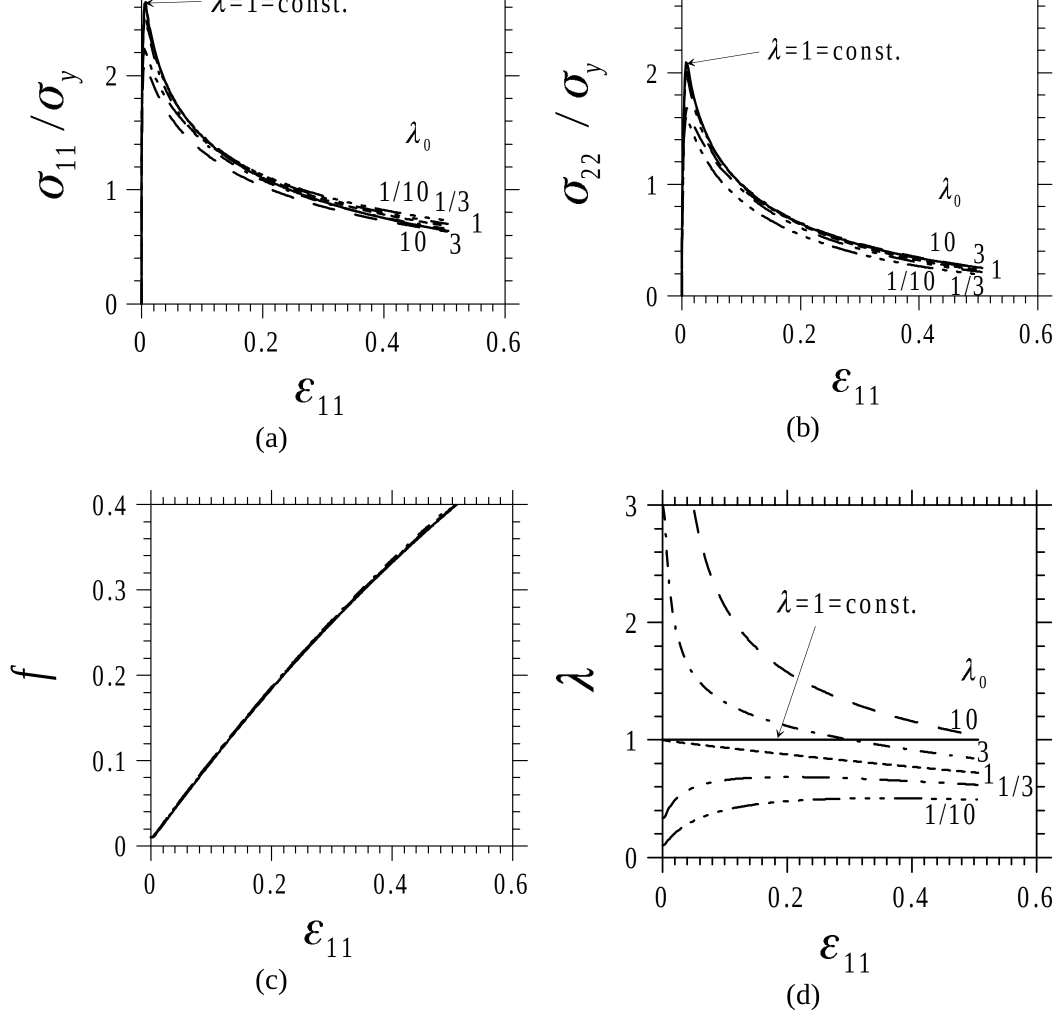

Figure 2. Effect of the initial aspect ratio λ_0 on the nonlinear response of orthotropic porous-plastic solids at $k_\epsilon = 0.0$. (a) nondimensional Cauchy stress σ_{11} vs logarithmic strain ε_{11}; (b) nondimensional Cauchy stress σ_{22} vs logarithmic strain ε_{22}; (c) void volume fraction f vs ε_{11}; (d) void aspect ratio λ vs ε_{11}

constitutive law.

In what follows results are presented in terms of components of the Cauchy stress tensor and of the logarithmic strain tensor aligned with reference axes x_1 and x_2. In order to manage nondimensional quantities, the current values of the stress components are normalized with respect to the uniaxial strength σ_y of the matrix material.

Assuming a strain-driven loading process, the nonlinear response of the constitutive law at a material point is represented under linear paths of the following type:

$$\varrho_2 - 1 = k_\epsilon(\varrho_1 - 1), \tag{3}$$

where: ϱ_1 and ϱ_2 are, respectively, the stretch ratios along reference axes x_1 and x_2; k_ϵ is a proportionality factor that define the slope of the path in the $\varrho_1 - \varrho_2$ plane. In the Introduction these paths have been defined quasi-radial: in fact they all depart from the undeformed state $\varrho_1 = \varrho_2 = 1$.

The initial void volume fraction, according to what explained in the Introduction, has been set equal to $f_0 = 0.01$ in the remainder of this Section.

Figure 2 shows the nonlinear model response under plane strain uniaxial deformation conditions with constrained lateral movements ($k_\epsilon = 0.0$). Results are presented in terms of: Cauchy stress vs logarithmic strain along the x_1 and x_2 reference axes (because of $\varepsilon_{22} = 0$ throughout the whole deformation process, σ_{22} is plotted here vs ε_{11}); evolution of the internal state variables f and λ in terms of

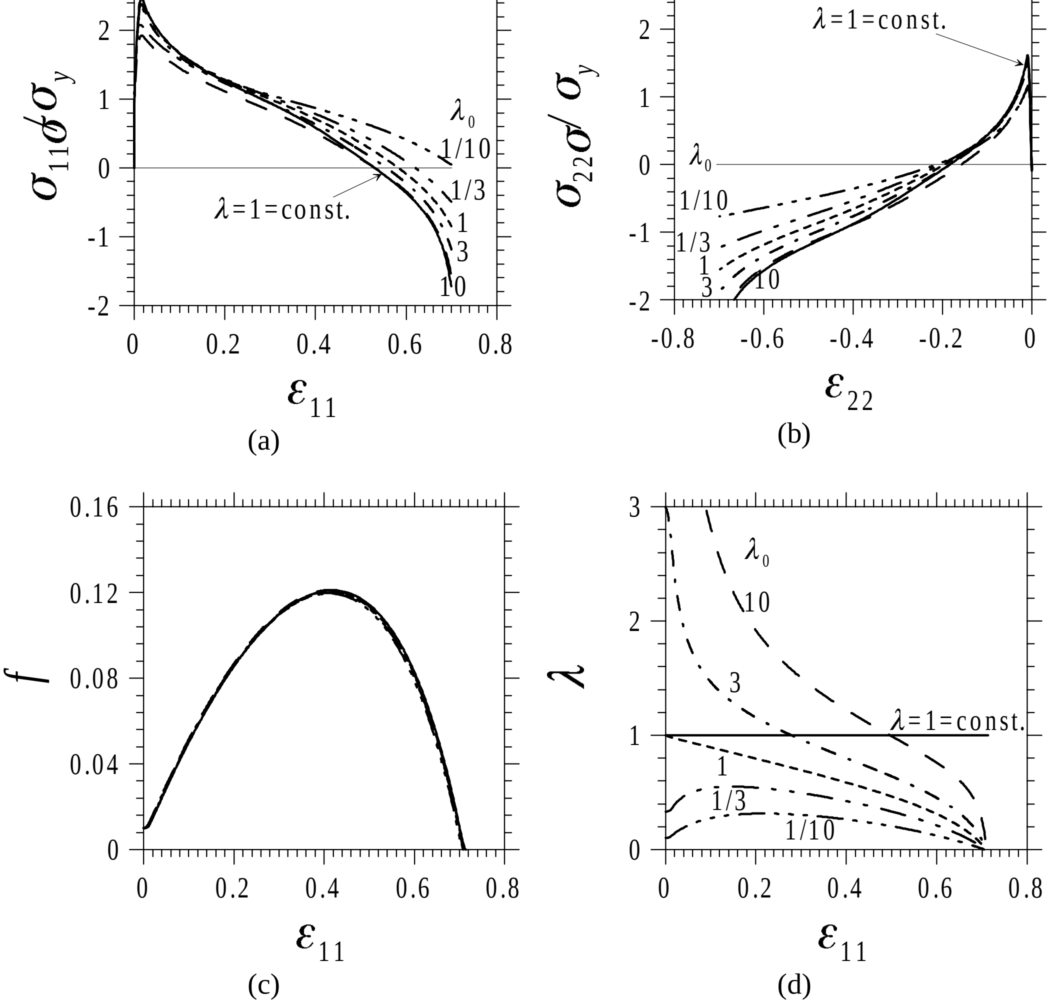

Figure 3. Effect of the initial aspect ratio λ_0 on the nonlinear response of orthotropic porous-plastic solids at $k_\epsilon = -0.5$. (a) nondimensional Cauchy stress σ_{11} vs logarithmic strain ε_{11}; (b) nondimensional Cauchy stress σ_{22} vs logarithmic strain ε_{22}; (c) void volume fraction f vs ε_{11}; (d) void aspect ratio λ vs ε_{11}

ε_{11}. These results are compared to those predicted by means of the transversely isotropic Gurson's model (named $\lambda = 1$=const. in the plots) in order to appraise the additional information gained by means of the enhanced orthotropic constitutive model. Various initialization values for λ, namely $\lambda_0 = 10, 3, 1, 1/3, 1/10$, have been adopted in order to explain the effect of voids with quite different initial shape on the behaviour of the fracture process zone. The results are plotted as long as $f \leq 0.4$: it is worth noticing that this extremely broad range (much wider than the range $f \leq 0.2$ discussed in the Introduction) has been checked only in order to show the performance of the constitutive model.

As far as the stress-strain relationships are concerned, λ_0 does not play a main role: only the peak stress values, beyond which softening takes place, appear to be significantly affected by λ_0; this aspect is discussed next.

Concerning the internal state variable evolution, it can be seen that f is only marginally affected by λ_0 while λ deserves a note. Even for $\lambda_0 < 1$, i.e. for $b_1 > b_2$ (see Fig. 1) the current value of λ has a tendency to approach the unitary value, that is the RVE deforms towards a circular cylindrical shape. Only for high ε_{11} values ($\varepsilon_{11} = 0.25 \div 0.3$ being a function of the λ_0 value) this tendency is reversed and λ decreases. This feature, which goes in the opposite way with respect to the expected one, is due to the coupled effect of transversely isotropic elasticity and plasticity.

Figure 3 shows similar results under simultaneous plane strain traction along the x_1 direction and compression along the x_2 direction ($k_\epsilon = -0.5$). The most remarkable effect can be appreciated from Fig. 3c: f starts increasing as soon as the elastic limit is crossed but, at $\varepsilon_{11} \cong 0.44$, it decreases due to the

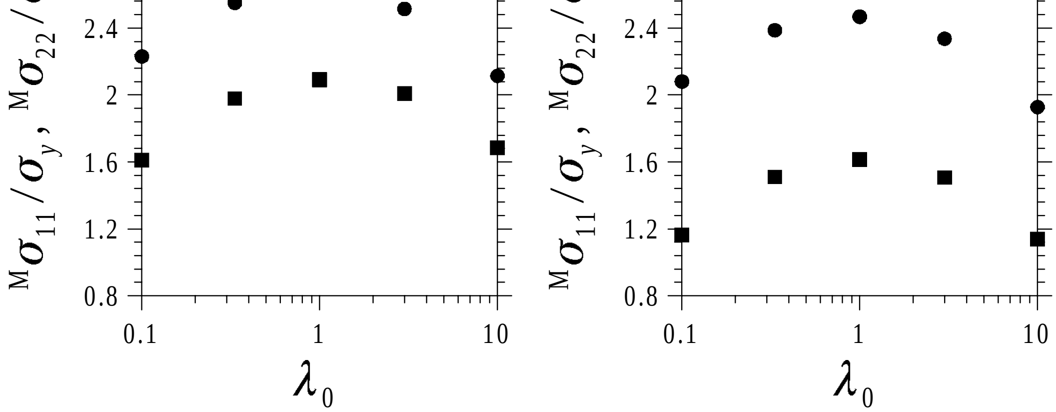

Figure 4. Effect of the initial aspect ratio λ_0 on the nondimensional peak values of Chauchy stresses ${}^M\sigma_{11}$ (circles) and ${}^M\sigma_{22}$ (squares). (a) $k_\epsilon = 0.0$; (b) $k_\epsilon = -0.5$

imposed deformation path. As a consequence the σ_{11} vs ε_{11} and σ_{22} vs ε_{22} plots show an hardening stage in compression due to $\dot{f} < 0$. Fig. 3d displays the major enhancement of the proposed model with respect to the Gurson's one: f vanishes at $\varepsilon_{11} \cong 0.71$ because λ tends to a null value, that is because the void assumes a needle-like shape. This feature cannot be modeled by means of the Gurson's model, for which $\lambda = 1$ at any deformation level.

Figure 4 collects plots of the nondimensional peak values of the Cauchy stresses σ_{11} and σ_{22} as a function of λ_0: for both $k_\epsilon = 0.0$ and $k_\epsilon = -0.5$ it can be seen that the range of initial aspect ratios here investigated can reduce by about 30% the values obtained by assuming a circular cylindrical RVE, thus leading to a more pronounced tendency to strain localization and subsequent fracture phenomena within anisotropic porous-plastic solids.

An important parameter to be considered in ductile tearing phenomena is the triaxiality stress ratio at the crack tip [12, 13], which can be defined as:

$$k_{triax} = \frac{\sigma_{eq}}{\sigma_h}, \tag{4}$$

where σ_{eq} is the Mises effective stress and σ_h is the hydrostatic stress. k_{triax} usually varies in the range $\frac{1}{3} \leq k_{triax} \leq 1$.

Figure 5 presents the evolution of k_{triax} along the imposed deformation paths considered above. It has to mentioned that the extremely high values of k_{triax} reached at the end of the deformation process characterized by $k_\epsilon = -0.5$ are due to the fact the σ_h approaches an almost null value.

Further results will be presented in a forthcoming paper in order to get insights into the coexisting phenomena of strain softening due to void growth and distortion and strain hardening due to the matrix constitutive law. Loading conditions at fixed k_{triax} will be also included in order to quantitatively evaluate the effect of non-circular void cross-section and of void distortion on the onset of strain localization in the fracture process zone that leads to the subsequent ductile tearing phenomenon.

ACKNOWLEDGMENTS

The work presented in this paper has been carried out in the framework of project PF MSTA II contract n^o 97.00906.PF34, funded by CNR (Italian National Research Council).

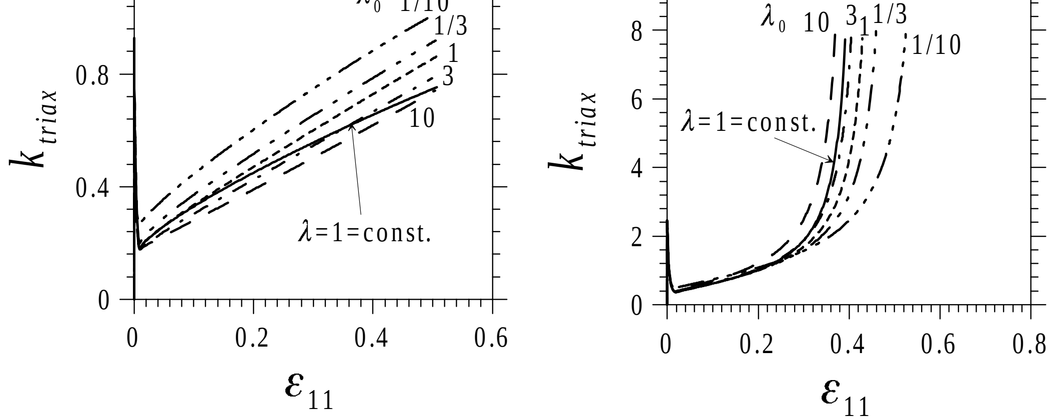

(a) (b)

Figure 5. Effect of the initial aspect ratio λ_0 on the evolution of the triaxiality parameter k_{triax}. (a) $k_\epsilon = 0.0$; (b) $k_\epsilon = -0.5$

REFERENCES

[1] A. L. Gurson. *ASME Journal of Engineering Materials and Technology*, 99:2–15, 1977.

[2] V. Tvergaard. Material failure by void growth to coalescence. *Adv. appl. Mech.*, 27:83–151, 1990.

[3] B. Dodd and Y. Bai. *Ductile fracture and ductility with applications to metalworking.* Academic Press, 1987.

[4] A Corigliano and S. Mariani. In S. R. Idelsohn, E. Oñate, and E. N. Dvorkin, editors, *Proceedings of the Fourth World Congress on Computational Mechanics*, Buenos aires (Argentina), 1998.

[5] S. Mariani. PhD thesis, Politecnico di Milano, 1998.

[6] S. Mariani and A. Corigliano. In T. Massard and A. Vautrin, editors, *Proceedings of the Twelfth International Conference on Composite Materials*, Paris (France), 1999.

[7] L. E. Malvern. *Introduction to the mechanics of a continuous medium.* Prentice-Hall, 1969.

[8] S. Nemat-Nasser and M. Hori. *Micromechanics: overall properties of heterogeneous materials*, volume 37 of *Applied mathematics and mechanics.* North-Holland, 1993.

[9] P. Suquet. In P. Suquet, editor, *Continuum micromechanics, CISM Courses and Lectures*, pages 197–264. Springer-Verlag, 1996.

[10] M. Gologanu, J.-P. Leblond, and J. Devaux. *Journal of the Mechanics and Physics of Solids*, 41:1723–1754, 1993.

[11] Q.-S. Zheng. *ASME Applied Mechanics Reviews*, 47:545–587, 1994.

[12] J. Koplik and A. Needleman. *International Journal of Solids and Structures*, 24:835–853, 1988.

[13] R. H. Dodds, C. F. Shih, and T. L. Anderson. *International Journal of Fracture*, 64:101–133, 1993.